

1 **Rainfall redistribution in subtropical Chinese forests changes over 22**
2 **years**

3 Wanjun Zhang^{a,b,c}, Thomas Scholten^c, Steffen Seitz^c, Qianmei Zhang^a, Guowei Chu^a, Linhua Wang^a,
4 Xin Xiong^{d,*}, Juxiu Liu^{a,*}

5
6 ^a*Key Laboratory of Vegetation Restoration and Management of Degraded Ecosystems, South China*
7 *Botanical Garden, Chinese Academy of Sciences, Guangzhou, 510650, China*

8 ^b*Key Laboratory of Urban Water Safety Discharge and Resource Utilization, Hunan University of*
9 *Technology, Zhuzhou, 412007, China*

10 ^c*Soil Science and Geomorphology, Department of Geosciences, University of Tübingen, Tübingen,*
11 *72070, Germany*

12 ^d*Lushan Botanical Garden, Chinese Academy of Sciences, Jiujiang 332900, China*

13

14 * Correspondence to: Juxiu Liu (ljxiu@scbg.ac.cn) and Xin Xiong (xiongx@lsbg.cn)

15 **Abstract**

16 Rainfall redistribution through the vegetation canopy plays a key role in the
17 hydrological cycle. Although there have been studies on the heterogeneous patterns of
18 rainfall redistribution in some ecosystems, the understanding of this process in different
19 stages of forest succession remains insufficient. Therefore, this study investigated the
20 change tendency of rainfall redistribution and rainwater chemistry in a subtropical
21 succession forest area in South China, based on 22 years (2001–2022) of monitoring
22 740 valid rainfall events. Results showed that at the event scale throughfall ratio showed
23 in order broadleaf forest (BF) < mixed forest (MF) < pine forest (PF), and stemflow
24 ratio showed in order BF > MF > PF. At the interannual scale, throughfall and stemflow
25 of forests experienced a decreasing followed by an increasing from 2001–2022 (except
26 stemflow of the pine forest), similar with the trend of open rainfall (except the mutation
27 time). The variability of throughfall presented in order MF (CV, 9.7%) < PF (11.8%) <
28 BF (16.4%), and variability of stemflow presented in order MF (CV, 38.6%) < PF (50.9)
29 < BF (56.2%). This suggested that changes of throughfall and stemflow in the broadleaf
30 forest were greater than those in the mixed forest and pine forest over time. Besides,
31 the difference of rainwater chemistry fluxes (TN, TP and K⁺) among the three forest
32 types were found and they changed in different order over time. On average, TN and
33 TP fluxes of throughfall presented in order BF < MF < PF, while K⁺ flux of throughfall
34 presented in order BF > MF > PF. Stemflow chemical fluxes varied less among forest
35 types and/or over time, though tree species exactly contribute to differences in stemflow
36 chemistry. The above results indicated that the patterns of rainfall redistribution
37 changed over time and showed characteristic variation driven by rainfall and forest
38 factors. This study provided insight into the rainfall redistribution process by linking
39 the long-term changing of rainfall pattern and subtropical forest succession sequence.

40 **Keyword:** throughfall, stemflow, variability, forest types, long-term

41 **1. Introduction**

42 In recent years, there has been on-going concern about the potential impacts of
43 climate change on forest ecosystems, particularly in terms of rainfall input associated
44 to water resource (Reynaert et al., 2020; Grossiord et al., 2017; Bruijnzeel et al., 2011;
45 Leuzinger and Körner, 2010). Numerous studies have documented rainfall regimes and
46 their effect on the water cycle in different regions of the world, including spatial and
47 temporal changes in the amount, intensity, and frequency (Brasil et al., 2018; Ponette-
48 González et al., 2010). Meanwhile, these variables in rainfall refer to the redistribution
49 of rainfall into canopy interception, throughfall and stemflow, being important
50 components of terrestrial ecosystems hydrological processes (Germer et al., 2010;
51 Levia and Frost, 2006; Loustau et al., 1992). Rainfall redistribution patterns can impact
52 the biogeochemistry cycle by affecting soil moisture distribution, which in turn affects
53 the activity of soil microorganisms that decompose organic matter (Tonello et al., 2021a;
54 Junior et al., 2017; Van Stan II and Pypker, 2015). The study of Sun et al. (2023) verified
55 that throughfall reduction significantly affected soil carbon cycle in a subtropical forest.
56 Therefore, understanding the roles of rainfall redistribution in the water cycle is
57 essential.

58 Rainfall redistribution, as the partitioning into interception loss, throughfall and
59 stemflow, is an important hydrological process that regulates water and nutrient cycling
60 in forest ecosystems. Interception loss refers to the part of the event rainfall intercepted
61 by the canopy, accounting for about 10%–30% of gross rainfall depending on the
62 studied forest canopy, such as shrub (Zhang et al., 2015), mixed broadleaf (Yan et al.,
63 2003), pine (Loustau et al., 1992). Later on, the remaining rainwater reaches the ground
64 either as throughfall or stemflow. Throughfall is a critical component of rainfall
65 redistribution, and it on average contributes to approximately 60%–90% of the gross
66 rainfall on the floor in forests, shrubland or cropland. (Zhang et al., 2023; Zhang et al.,
67 2021; Brauman et al., 2010; Marin et al., 2000). Raindrops coalesce or splash on canopy
68 leaf surfaces, generating spatially different throughfall volume and raindrop kinetic
69 energies which can be larger or lower than that of open rainfall (Levia et al., 2019;
70 Goebes et al., 2015). Stemflow, the left rainwater flowing bottomwards along the plant
71 stem or trunk, often accounts for only a small proportion (0–12%) of rainfall (Niu et al.,
72 2023; Yue et al, 2021; Llorens and Domingo 2007). Nevertheless, stemflow inputs can
73 be important as hot spots for near-trunk soils, inducing water and nutrient enrichment
74 and deep infiltration, but also erosion (Zhao et al., 2023; Llorens et al., 2022). It can

75 funnel more water than open rainfall on an equivalent area and contributes to 10% of
76 the annual soil water input (Levia and Germer, 2015; Chang and Matzner, 2000).
77 Throughfall and stemflow restrict water input to the soil layer, thereby affecting soil
78 moisture conditions, runoff generation and water and nutrient cycling (Lian et al., 2022;
79 Lacombe et al., 2018; Klos et al., 2014).

80 The proportions of rainfall redistribution are generally driven by meteorological
81 conditions (e.g., rainfall amount, intensity, duration) and vegetation cover (e.g., canopy
82 structures, tree characteristics) (Tonello et al., 2021a; Sun et al., 2018; Muzyło et al.,
83 2012; Nanko et al., 2006). For meteorological conditions, numerous studies have
84 documented that throughfall volume and stemflow volume increase with increasing
85 gross rainfall and intensity (Ji et al., 2023; André et al., 2011). The ratios of throughfall
86 and stemflow were both characterized with logarithmically increasing with rainfall,
87 tending to be quasi-constant for heavy rainfall events (Zhang et al., 2021; Liu et al.,
88 2019). This was also synchronously related to the gradual saturation of the canopy
89 which limited the ratios of rainwater partitioning (Carlyle-Moses et al., 2004). Besides,
90 differences of water volume spatially exist from place to place. The spatial variability
91 (expressed as a coefficient of variation) of throughfall volume is generally higher for
92 small rainfall events (< 10 mm) than that for heavy rainfall events (Germer et al., 2006;
93 Price et al., 1997).

94 Rainfall redistribution among different plant species can vary significantly due to
95 differences in the structure and characteristics of their canopies. In special, some of the
96 key factors determine the redistribution of rainfall, for example, leaf area index (LAI),
97 leaf shapes and orientations can affect the amount of intercepted loss and throughfall
98 (Zhang et al., 2021; Goebes et al., 2015; Keim et al., 2006). The diameter at breast
99 height (DBH), bark type and orientation of trunks/stems and branches influence the
100 amount of stemflow (Levia et al., 2015; Livesley et al., 2014; Germer et al., 2010). For
101 each of the rainfall partitioning fluxes, their responses to the influential predictors often
102 show high variation. A modelling study of rainfall partitioning in China explained that
103 throughfall was best represented by mean tilt angle (MTA), followed by DBH.
104 Subsequently, DBH was the dominant predictor for stemflow, followed by LAI and
105 bark texture (Zhang et al., 2023). Due to these factors, rainfall redistribution presented
106 different degrees of spatial variability. This variability (expressed as coefficient of
107 variation) decreased with increasing rainfall amount and intensity, consequently
108 tending to be quasi-constant (Germer et al., 2006). Besides, at interannual scale, ratios

109 of rainfall redistribution are driven by annual canopy structures. The study of Niu et al.
110 (2023) documented that annual throughfall ratio gradually increased, while annual
111 stemflow ratio and interception loss ratio decreased with increasing thinning intensity
112 in shrub plantation. Meanwhile, annual changes of rainfall events (amount and intensity)
113 reinforced the time instability of throughfall spatial variability (Rodrigues et al., 2022).
114 Overall, the rainfall-canopy interactions play a key role in rainfall redistribution
115 processes and further affect the water cycle in many ecosystems.

116 Vegetation canopy is the functional interface between ecosystem and atmospheric
117 wet deposition (Van Stan II and Pypker, 2015). The leaf and trunk/stem, acting as a
118 filter, alter rainwater chemical concentrations via leaching and depositing processes. As
119 a result, throughfall and stemflow exhibit high chemical concentrations compared to
120 the open rainfall (Jiang et al., 2021; Zimmermann et al., 2007). For instance, in a Chinese
121 pine plantation, the volume weighted mean concentrations of NH_4^+ and NO_3^- in
122 throughfall were significantly higher than those in open rainfall (Wang et al., 2023).
123 Stemflow ion fluxes (e.g., K^+) from deciduous tree species were greater than those for
124 evergreen tree species because of the differences in bark morphology and branch
125 architecture (Su et al., 2019). Moreover, it is also common that throughfall and
126 stemflow chemistry fluctuated seasonality with the shifts in rainfall regime and leaf
127 growth (Turpault et al., 2021; Siegert and Levia, 2014; Staelens et al., 2007). A large
128 number of elements required by plants are mainly N, P, K, Ca and Mg. In general, N, K
129 and Ca are the most important inputs to forest ecosystem, and P is the least. Phosphorus
130 (P) is considered to be a limiting nutrient element in tropical and subtropical forests.
131 The long-term productivity of vegetation depends on the input of atmospheric P.
132 Besides, the increasing trend in seasonal drought and atmospheric nitrogen (N)
133 deposition in subtropical areas of China were reported (Zhou et al., 2011), and may
134 inhibit the growth of plant and affect productivity and functioning of forest ecosystems
135 (Wu et al., 2023; Borghetti et al., 2017). Therefore, the important significance of
136 atmospheric precipitation to the ecosystem can also be seen from the amount of element
137 cycling, and canopy leaching also plays an important role in the chemistry cycle of
138 forest ecosystems.

139 Although there have been studies on the spatio-temporal variability of rainfall
140 redistribution, most of these are limited to data of short-term monitoring over one-two
141 years or several months (Liu et al., 2019; Ziegler et al., 2009; Carlyle-Moses, 2004;
142 Marin et al., 2000). There are few studies exceeding several years experiments and

143 focusing on forest structural changes and rainwater interception (Grunicke et al., 2020;
144 Shinohara et al., 2015; Jackson, 2000). Long-term field monitoring studies are
145 considered to be valuable to gain insight into the temporal dynamics of forest
146 hydrological processes (Rodrigues et al., 2022; Sun et al., 2023; Levia and Frost, 2006).
147 Such studies can also contribute to identify patterns and trends in rainfall redistribution,
148 which is essential for predicting the long-term effect of water resource change on forest
149 ecosystems.

150 Therefore, in this study, we focus on the changing characteristics of throughfall
151 and stemflow in a subtropical forest succession sequence (pine forest→mixed forest→
152 monsoon evergreen broadleaf forest), based on long-term monitoring. Specifically, the
153 objectives are to analyze: (1) the changes of water volume of throughfall and stemflow
154 among the three forests, (2) the changes of water chemistry (TN, TP, K⁺) of rainfall,
155 throughfall and stemflow among the three forests. We hypothesize that: (1) both
156 throughfall and stemflow in the broadleaf forest were characterized with high
157 variability compared to mixed forest followed by pine forest, (2) chemistry flux of
158 throughfall and stemflow changed over time with in order broadleaf forest > mixed
159 forest > pine forest. We aim to assess the variability of forest hydrological processes
160 from a long-term perspective to help predict future dynamic trends of water resources
161 in subtropical forest ecosystems.

162

163 **2. Materials and Methods**

164 *2.1. Study site*

165 This study was conducted at the Dinghushan Biosphere Reserve (23°09' 21" N ~
166 23°11' 30" N, 112°30' 39" E ~ 112°33' 41" E) located in Zhaoqing City, South China.
167 Dinghushan catchment consists of two streams both with 12 km length, which flow into
168 the West River (the main trunk of the Pearl River). According to the Köppen-Geiger
169 climate classification (Kottek et al., 2006), the study area belongs to tropical monsoon
170 climate (Cwa) with pronounced wet (April-September) and dry season (October-
171 March). The average annual temperature is 20.9 °C, and the annual rainfall and
172 evaporation are 1900 mm and 1115 mm, respectively. Dinghushan Biosphere Reserve
173 is covered with a complete horizontal succession series of three types of subtropical
174 forest, which is highly representative of the region (Zhou et al., 2011). Monsoon
175 evergreen broadleaf forest (BF) is 400 years old with typical tree species including

176 *Castanopsis chinensis* (Spreng.) Hance, *Schima superba* Gardner & Champ.,
177 *Cryptocarya concinna* Hance, etc. The mixed pine/broadleaf forest (MF) is a natural
178 succession with a coniferous broadleaf ratio of about 4:6, and 70–80 years old. The
179 main broadleaf tree species are *Schima superba* Gardner & Champ., *Castanopsis*
180 *chinensis* (Spreng.) Hance, and the coniferous species *Pinus massoniana* Lamb. The
181 pine forest (PF) planted before 1960 belongs to the primary succession community
182 where *Pinus massoniana* Lamb forms the only tree layer. The community composition
183 and biodiversity are shown in Table S1.

184

185 2.2. Gross rainfall, throughfall and stemflow monitoring

186 Atmospheric rainfall data was collected at Dinghushan Automatic Meteorological
187 Station from 2001–2022. Automatic meteorological systems were used to measure
188 atmospheric pressure (DPA501 gas-pressure meter), temperature (HMP45D sensor),
189 relative humidity (HMP45D sensor), rainfall (SM1-1 pluviometer), etc. Datalogger
190 (America Campbell, CR1000X) was used to control measurement sensors and store
191 meteorological data. The resolution of data recording was ± 0.2 mm with a time interval
192 of 10 min. The raw data comprised annual rainfall amounts, as well as single rainfall
193 events with throughfall and stemflow measurements.

194 Throughfall and stemflow were collected in all three forest types and
195 synchronously measured. Devices with cross-shaped collectors (1.25 m²) attached to
196 reservoirs (1000 L) at the bottom were used to collect throughfall. Three throughfall
197 devices were randomly installed in each forest field (Fig. S1).

198 Half-shell plastic tubes were installed around tree trunks attached to reservoirs
199 (1000 L) at the bottom to collect stemflow. The ratio of volume (mL) to canopy area
200 (cm²) is the stemflow (mm). A total of 24 trees were selected to measure stemflow
201 volume (Table S2). In detail, four tree species were selected in the broadleaf forest,
202 including *Acmena acuminatissima* (Blume) Merr. et Perry (SF1), *Cryptocarya*
203 *chinensis* (Hance) Hemsl. (SF2), *Gironniera subaequalis* Planch. (SF3), *Schima*
204 *superba* Gardn. et Champ. (SF4), with 3 repetitions respectively. Three tree species
205 were selected in the mixed forest, including *Castanea henryi* (Skam) Rehd. et Wils.
206 (SF5), *Schima superba* Gardn. et Champ. (SF6), *Pinus massoniana* Lamb. (SF7), with
207 3 repetitions respectively. In the pine forest, *Pinus massoniana* Lamb. (SF8) was
208 selected as the monitoring subject with 3 repetitions.

209

210 2.3. Rainwater chemistry measurement

211 For the measurement of rainwater chemistry, rainwater samples were from 2000,
212 2010 and 2022 in Dinghushan area. The samples of open rainfall, throughfall and
213 stemflow were manually collected for every one-month period, respectively. The
214 samples of open rainfall and throughfall were collected with three repetitions,
215 respectively and stemflow with four repetitions in the broadleaf forest, three repetitions
216 in the mixed forest and three repetitions in the pine forest. In total, 792 rainwater
217 samples (108 open rainfall, 324 throughfall and 360 stemflow) were collected.

218 Rainwater samples were defrosted and filtered through 0.45 μm polypropylene
219 membranes. Concentrations of total nitrogen (TN) and total phosphorus (TP) were
220 measured using ultraviolet spectrophotometer (Lambda 25, Perkin-Elmer), and ion
221 potassium (K^+) was measured using an inductively coupled plasma optical emission
222 spectrometer (Optima 2000, Perkin-Elmer), respectively. The origin data of TN, TP and
223 K^+ were processed into annual flux and monthly values by weighted average method,

$$224 \quad C = \frac{\sum C_i * V_i}{\sum V_i} \quad (1)$$

225 where C_i and V_i are the concentrations of ions (mg L^{-1}) and water sample volume (L) in
226 each rainfall event, respectively.

227

228 2.4. Other measurement and statistical analysis

229 In the forests, plant density and canopy structure have been measured every five
230 years since 2000. 25 plots of 20 m \times 20 m (A1-A25 plots) were built on a plot of 1 hm^2
231 to survey tree density (Fig. S1). Then, 25 plots of 5 m \times 5 m (B1-B25 plots) were
232 randomly set on the A1-A25 plots to survey shrub density. Finally, 25 plots of 1 m \times 1
233 m (C1-C25 plots) were randomly set on the B1-B25 plots to survey herb density. The
234 percentage of the surface area covered by plants to the total plot area is termed canopy
235 coverage (%). 25 observation plots (1 m \times 1 m) were selected in the 1 hm^2 area of each
236 forest type. LAI (Leaf area index) was measured using a LAI-2200 plant canopy
237 analyzer with 90° view caps (Li-Cor Inc., USA). 10 observation points (distance about
238 10 m) were selected in the 1 hm^2 area of each forest type with 5 replications. Growth
239 indicators of the selected trees have been recorded: tree height (m), diameter at breast
240 height (DBH, cm), and crown area (CA, m^2). Tree height was measured using laser
241 range finder. Tape measure was used to measure the diameter of trees at a height of 1.3

242 m, namely DBH. CA: the laser rangefinder was used to measure the maximum diameter
243 at the edge of the canopy, with multiple measurements at different points to ensure
244 accuracy.

245 The differences in throughfall and stemflow among different forests were assessed
246 using analysis of variance (ANOVA), followed by a Tukey test for multiple
247 comparisons between means. Mann-Kendall (MK) test was used to analyze the
248 variation trend of annual rainfall. All statistical procedures were conducted with $\alpha =$
249 0.05 threshold for significance, in the IBM SPSS statistics 22.0 software (IBM Inc.).

250

251 **3. Results**

252 *3.1. Rainfall and temperature characteristics*

253 Based on the 22 years rainfall dataset from the Dinghushan area, annual gross
254 rainfall ranged between 1370.0 and 2361.1 mm (Fig. 1). 78.0% of gross rainfall
255 appeared in the wet season (April–September). Result of M-K test showed that rainfall
256 was in a significantly decreasing trend from 2001–2007 ($UF < 0, P < 0.05$), and shifted
257 into a significantly increasing trend from 2012–2022 ($UF > 0, P < 0.05$). Moreover,
258 2008 and 2011 (the intersection of UF and UB) were the mutation time of rainfall trend
259 ($P < 0.05$). Anomaly were revealed in the temporal variability (coefficient of variation,
260 CV of 16.6%) in annual rainfall (Fig. 1a). Anomaly varied at -426.4–476.8 mm and -
261 258.0–471.4 mm in the wet season and dry season, respectively. By comparison, dry
262 season experienced greater variation with CV of 40.4% than wet season with CV of
263 21.7%. Besides, annual raining days obviously tended to decrease over time from 2012
264 to 2021(Fig. 1b). Based on five rainfall classifications, it was shown among 22 years
265 that rainfall < 10 mm account for about 68.5% of total raining days (2856), while
266 rainfall > 50 mm account for about 4.9%. Besides, annual temperature changed between
267 21.8 °C and 23.3 °C over 22 years. Result of M-K test showed statistically significant
268 rising trend for temperature for 8 years out of 22 years ($UF > 0, P < 0.05$). Moreover,
269 2005 and 2013–2014 were the mutation time of temperature trend ($P < 0.05$).

270

271 *3.2 Variability of throughfall*

272 Rainfall redistribution (throughfall and stemflow) among the three forests all
273 experienced differing magnitude during 22 years (Fig. 2). Annual throughfall were
274 concentrated between 954.2 mm and 2192.6 mm. Result of M-K test showed that

275 throughfall was in a significantly decreasing trend at first ($UF < 0$, $P < 0.05$) and then
276 shifted into an significantly increasing trend ($UF > 0$, $P < 0.05$) from 2001–2022,
277 similar with the trend of open rainfall. Differently, the mutation of throughfall trend
278 occurred in 2008, 2011 and 2021 in the broadleaf forest, 2008 and 2011 in the mixed
279 forest, 2006, 2008, 2011 and 2021 in the pine forest ($P < 0.05$). For throughfall ratio,
280 it varied significantly both at the event and interannual scales (Fig. 3a, b and c). The
281 median of annual throughfall ratio in the broadleaf forest varied between 60% and 120%
282 with CV of 16.4% from 2001–2022. The median of throughfall ratio in the mixed pine
283 and broadleaf forest varied between 80% and 110% with a CV of 9.7%. The median of
284 throughfall ratio in the pine forest varied between 59% and 110% with a CV of 11.8%.
285 Therefore, throughfall ratio was characterized by a relatively low variability over
286 annual-time scale ($CV < 20\%$). Besides, some differences of throughfall ratio were
287 found among the three forest types based on rainfall classifications (Fig. 3d). For
288 rainfall events < 10 mm, throughfall ratio range in the broadleaf forest was 30%–70%,
289 while in the other two forest types it was 15%–85%. The mean value of throughfall
290 ratio was relatively small in the broadleaf forest (53.9%), though no significant
291 difference among the three forests ($P > 0.05$) were detected. For rainfall events < 50 mm,
292 no significant difference of throughfall ratio among the three forest types was found ($P >$
293 0.05). However, the median values of throughfall ratio in the pine forest (90.0%) and
294 the mixed forest (89.4%) were both significantly larger than that in the broadleaf forest
295 (83.7%) for rainfall events > 50 mm.

296 CV values of throughfall based on all the rainfall event classifications were drawn
297 in the Fig. 4a. Results showed that median CV of throughfall in the pine forest (15.2%)
298 was lower than that for the broadleaf forest (21.7%) and for the mixed forest (26.3%)
299 for rainfall events < 10 mm. For rainfall events > 10 mm, small differences of median
300 CV among the three forest types were shown. Meanwhile, CV values decreased with
301 the increasing rainfall events, eventually falling to 3.5%–4.3%. Besides, CV values of
302 throughfall based on interannual scale were drawn in the Fig. 5a, b and c. Annual CV
303 values among different forest types showed different fluctuations over time. The
304 medians of CV in annual, wet and dry seasons presented different order in different
305 years. According to linear fitting, significant negative correlations were found in the
306 median of CV_{TF} in the mixed forest over time ($r = 0.63$, $P < 0.01$). In addition, fitting
307 result of in total 740 rainfall events in 22 years showed that CV values of throughfall
308 significantly decreased with increasing gross rainfall (Fig. S2).

309

310 3.3 Variability of stemflow

311 Annual stemflow was concentrated between 9.0 and 119.7 mm over 22 years (Fig.
312 2). More stemflow were collected in the broadleaf forest and mixed forest than in the
313 pine forest. Result of M-K test showed that stemflow of both broadleaf forest and mixed
314 forest were in a decreasing trend at first ($UF < 0$, $P < 0.05$) and then shifted into an
315 increasing trend ($UF > 0$, $P < 0.05$), different from continuously increasing trend of
316 pine forest ($UF > 0$). The mutation of stemflow trend occurred in 2008 in the broadleaf
317 forest, 2011 in the mixed forest, 2006, 2012 and 2015 in the pine forest ($P < 0.05$).
318 Stemflow ratio changed significantly both at the event and interannual scales (Fig. 3a,
319 b and c). Among 22 years, the median of annual stemflow ratio in the broadleaf forest
320 varied between 1.3% and 5.4% with a CV of 56.2%. The stemflow ratio of mixed forest
321 varied between 1.5% and 4.4% with a CV of 38.6%. In the pine forest, it varied between
322 0.3% and 1% with a CV of 50.9%. This indicated that the stemflow ratio was
323 characterized by an extremely high variability over time. Same to the seasonal
324 throughfall ratio, the medians of stemflow ratio in annual, wet and dry seasons
325 presented different orders in different years. Besides, the stemflow ratio significantly
326 changed among tree species and among rainfall classifications (Fig. 3e). By comparison,
327 stemflow ratios of the SF1 and SF2 trees in the broadleaf forest were both higher in all
328 the tree species for the rainfall events < 50 mm. However, for strong events (> 50 mm),
329 the stemflow ratio of the SF5 tree in the mixed forest was highest for all tree species,
330 followed by the trees in the broadleaf forest. For all the rainfall events, the stemflow
331 ratio of SF7 in the mixed forest and SF8 in the pine forest were both lower than that for
332 other tree species.

333 CV values of stemflow based on rainfall event classifications were drawn in the
334 Fig. 4b. By comparison, stemflow varied more than those of throughfall across rainfall
335 events, with CV_{SF} values of 25%–130%. Median CV of stemflow in the pine forest was
336 always lower (45%–68%) than that for the other two forest types (56%–120%). CV
337 values of stemflow based on interannual scale changed over time among different forest
338 types (Fig. 5d, e and f). The medians of CV_{SF} in annual, wet and dry seasons presented
339 different order in different years. By comparison, CV_{SF} was always greater than CV_{TF} ,
340 and interannual fluctuation of CV_{SF} was also stronger than CV_{TF} . According to linear
341 fitting, significant negative correlations were found in the median of CV_{SF} in the
342 broadleaf forest over time ($r = 0.73$, $P < 0.001$). In addition, fitting result of in total

343 740 rainfall events in 22 years showed that *CV* values of stemflow both significantly
344 decreased with increasing gross rainfall (Fig. S2).

345

346 3.4. Rainwater chemistry

347 Rainwater (open rainfall, throughfall and stemflow) chemical properties (TN, TP
348 and K^+ concentration) were measured in the three forest types, respectively. All of TN,
349 TP and K^+ values presented in order stemflow > throughfall > open rainfall (Fig. 6a, b
350 and c). However, changes of TN, TP and K^+ were different for the three forest types
351 among 2000, 2010 and 2022. For instance, in 2000 and 2010, TN values of throughfall
352 and stemflow decreased for both in order of pine forest > mixed forest > broadleaf forest,
353 while no such result could be confirmed in 2022. Similarly, TP values of throughfall in
354 broadleaf forest was 1.3 times higher than that in pine forest in 2022, while TP values
355 in pine forest was 6.8 times than that in broadleaf forest in 2000. K^+ values of stemflow
356 in 2010 (6.76 mg L^{-1}) and 2022 (6.22 mg L^{-1}) were higher for broadleaf forest than
357 those for pine forest (3.76 mg L^{-1} and 2.46 mg L^{-1}), which was different from that in
358 2022.

359 TN, TP and K^+ fluxes of stemflow were $< 10 \text{ kg ha}^{-1} \text{ a}^{-1}$, $0.2 \text{ kg ha}^{-1} \text{ a}^{-1}$, 6 kg ha^{-1}
360 a^{-1} , respectively, all lower than those of throughfall and open rainfall (Fig. 7d, e and f).
361 In the 2000, 2010 and 2022, TN flux ($39.4\text{--}87.4 \text{ kg ha}^{-1} \text{ a}^{-1}$) was 1.2–1.8 times greater
362 than that of open rainfall, 3.3–28.0 times greater than that of stemflow. TP flux (1.1--
363 $2.7 \text{ kg ha}^{-1} \text{ a}^{-1}$) was 1.0–2.3 times greater than that of open rainfall, 8.7–31.4 times
364 greater than that of stemflow. K^+ flux ($21.5\text{--}59.2 \text{ kg ha}^{-1} \text{ a}^{-1}$) was 2.2–8.1 times greater
365 than that of open rainfall, 2.2–26.8 times greater than that of stemflow. In addition, TN,
366 TP and K^+ fluxes of stemflow increased with succession from primary to climax,
367 namely pine forest < mixed forest < broadleaf forest. Different from this, differences in
368 chemistry fluxes of throughfall was not found among different forests, neither among
369 different periods.

370 Besides, monthly chemistry concentrations in rainfall, throughfall and stemflow
371 showed distinct changes (Fig. 7). Monthly TN, TP and K^+ concentrations of rainfall
372 were always lower than those of stemflow for all trees. Monthly TN, TP and K^+ of
373 stemflow in the dry season were generally higher than in the wet season. High monthly
374 TN concentrations of stemflow with SF6 of mixed forest and SF8 of pine forest were
375 found, especially in dry season with maximum TN concentrations of 27.59 mg L^{-1} at

376 SF6 and 19.94 mg L⁻¹ at SF8, respectively. Differently, high monthly K⁺ concentration
377 of stemflow at SF4 in broadleaf forest was found, with in dry season maximum K⁺
378 concentration of 25.17 mg L⁻¹.

379

380 **4. Discussion**

381 *4.1. Open rainfall partitioned to throughfall and stemflow*

382 Studies in forests have confirmed that throughfall volume increased with
383 increasing gross rainfall at event scale, accounting for 60%–80% of gross rainfall (Ji et
384 al., 2023; André et al., 2011; Carlyle-Moses, 2004). Throughfall ratio changed over time
385 and showed different fluctuations among different forests (Fig. 3). During light rainfall
386 events with rainfall amounts <10 mm, a low proportion of raindrops would reach the
387 ground as throughfall, as the tree canopy intercepts almost all the incoming raindrops.
388 Specifically, high canopy coverage in broadleaf forest can reinforce raindrop intercept
389 (Brasil et al., 2018; Ponette-González et al., 2010), consequently generating lower
390 throughfall ratio than those in the mixed forest and pine forest (Fig. 3). During moderate
391 rainfall events (10–50 mm), given that the intercept effect of the wetting tree canopy
392 was weakened (Shinohara et al., 2015), throughfall ratio was in a high and steady state.
393 As the gross rainfall increases further (>50 mm), significant differences of throughfall
394 ratio were found among the three forests. Throughfall ratio was significantly lower in
395 the broadleaf forest than those in the other two forests. Likewise, such differences due
396 to rainfall event class also appeared in other forest studies with stands such as beech,
397 pine in monocultures and mixed pine-beech (Blume et al., 2022). Influenced by forest
398 stand characteristics, throughfall therefore indicated different forest water budget.

399 Stemflow of forests were variably controlled by tree species, on average
400 accounting for about <10% of gross rainfall, even lower (<1%) (Sun et al., 2018; André
401 et al., 2008; Crockford and Richardson, 1990). In our study site, the lowest stemflow
402 (<1%) was collected in the pine forest, though weakly increasing with rainfall
403 classifications (Fig. 3). Stemflow ratio in broadleaf forest was maintained at 5%–10%
404 without the effect of rainfall amount seemingly. In detail, stemflow ratio of pine forest
405 (SF8) was significantly lower than those of broadleaf forest (SF1~4). And in the mixed
406 forest, broad-leaved trees (SF5 and SF 6) have larger stemflow than pine tree (SF7).
407 However, for some rainfall events, extraordinary low proportion of stemflow in the
408 broadleaf forest and extraordinary high proportion in the pine forest were caught. This

409 implied the key role of rainfall conditions (e.g., intensity, duration) and tree species with
410 tree traits (e.g., branch angle), consistent with reported studies e.g., in evergreen forest
411 (Chen et al., 2019; Bruijnzeel et al., 2011) and pine forest (Pinos et al., 2021; Crockford
412 and Richardson, 1990). Moreover, ANOVA showed significant differences of stemflow
413 ratio among tree species and rainfall classifications ($P < 0.001$) (Table 1). This indicated
414 that rainfall and tree species simultaneously affect stemflow. Branch inclination angle,
415 canopy cover, tree height and DBH of tree species proved to be key factors in stemflow
416 yield (Levia et al., 2015).

417 Throughfall and stemflow were generally enriched in chemical concentration
418 compared with open rainfall due to leachable canopy/stem ion pools (Jiang et al., 2021;
419 Van Stan et al., 2017; Zimmermann et al., 2007). In our study, the concentration of K^+
420 in stemflow was 16 times higher than that in open rainfall and in throughfall reached
421 up to 11 times higher than open rainfall (Fig. 6). Similar results were also found in
422 artificial plantation (*Acacia mangium* and *Dimocarpus longan*) of South China (Shen
423 et al., 2013), in Oriental beech (*Fagus orientalis* Lipsky) trees in Northern Iran (Moslehi
424 et al., 2019), indicating strong K^+ leaching from canopy. Even so, throughfall was
425 generally characterized with high fluxes compared to open rainfall followed by
426 stemflow, it thus is the largest contributor to wet deposition. Meanwhile, TN flux of
427 throughfall was greatest in the pine forest in 2010, TP flux of throughfall was greatest
428 in the broadleaf forest in 2000, and K^+ flux of throughfall was greatest in the mixed
429 forest in 2010. It should be noted that the differences of rainwater chemistry shifted
430 over time among the three forests. Accordingly, throughfall and stemflow via canopy
431 and stem input soil is a significant contributor, and its long-term effect on ecosystems
432 needs more attention (Fan et al., 2021). After all, atmospheric wet deposition provides
433 nutrient requirement for ecosystems, but also imposes a considerable burden on the
434 ecosystems in general. For instance, N enrichment and P limitation have proven to have
435 different effect on soil carbon sequestration, microbial community composition and
436 forest productivity, especially in tropical and subtropical forest ecosystems with highly
437 weathered soils (Zheng et al., 2022; Li et al., 2016; Huang et al., 2012). Besides,
438 throughfall and stemflow was mainly characterized by low chemical concentrations in
439 the wet season and high concentrations in the dry season. Primary reasons for seasonal
440 rainwater chemistry may be attributable to moisture source associated with frontal
441 weather systems and gradually depleting effect with increasing rainfall amount
442 (Dunkerley, 2014; Germer et al., 2007). The present study in subtropical forests and

443 previous studies in tropical forests and European temperate forests all exhibited variable
444 rainwater chemistry in throughfall and stemflow, both spatially and temporally
445 (Zimmermann et al., 2007; Staelens et al., 2006; Seiler and Matzner, 1995). In fact, the
446 chemical concentration of rainfall redistribution was also affected profoundly by
447 canopy and stem parameters of tree species (Tonello et al., 2021b; Chen et al., 2019).
448 In our study, some differences of TN, TP and K^+ were also found among SF1~SF8 due
449 to tree-species specific effect (Legout et al., 2016; De Schrijver et al., 2007).

450

451 *4.2. Long-term changes of rainfall in forests*

452 Rainfall regimes induce divergent spatially hydrological changes (Wu et al., 2024).
453 Likewise, our study found that throughfall of forests experienced a decreasing followed
454 by an increasing from 2001–2022, similar with the trend of open rainfall, and stemflow
455 showed characteristic trends in different forests especially in the pine forest (Fig. 1).
456 This suggested that the complexity of forest structure and rainfall amount and their
457 change exacerbated the spatio-temporal variability of throughfall and stemflow. Firstly,
458 interannual variability of forest structure (e.g., canopy coverage, leaf area index) and
459 tree parameters (e.g., height, DBH and CA) made throughfall and stemflow distribution
460 uncertain (Yue et al., 2021). From 2001 to 2022, changes in forest structure were
461 confirmed in all three forests, such as changes in plant density, canopy coverage and
462 LAI (Fig. 8). Throughfall ratio and stemflow ratio in the succession forest systems all
463 varied over time accordingly. Similarly, driven by forest structure (e.g., tree density,
464 species dominance), a six-year dataset from the Brazilian Atlantic Forest showed that
465 the spatial variability of throughfall over time was less stable (Rodrigues et al., 2022).
466 Besides, the variation of stemflow (CV_{SF}) was obviously larger than that of throughfall
467 (CV_{TF}) (Fig. 4), which probably was attributed to the differences of tree species in
468 stemflow (Fig. 3). For a forest succession, a 17 years' study showed that the shift from
469 monoculture Japanese red pine to mixture of red pine, evergreen oak and theaceous tree
470 made stemflow significantly increasing (Iida et al., 2005). Likewise, for the forest
471 succession in Dinghushan area, stemflow ratio in broadleaf forest and mixed forest were
472 both higher than that in tree-monospecific pine forest. High plant density (tree and shrub)
473 and LAI in broadleaf forest and mixed forest conduce to rainwater interception of multi-
474 canopy trees through more leaves and angled branches, which potentially enhanced
475 stemflow (Fig. 8). Indeed, some differences of rainfall redistribution appeared in multi-
476 layered vegetative structure. An experiment on vegetation communities with a complex

477 multi-layered structure found that interception loss from shrubs was two-times higher
478 than from trees, and smaller trees generated stemflow more efficiently than the higher
479 ones (Exler and Moore, 2022). Based on the 22 years' data from forest community
480 survey in our study site, forest canopy parameters (e.g., coverage and LAI) of trees and
481 shrubs showed variation over time from 2001 to 2022 (Fig. 8). In the broadleaf forest,
482 plant density of trees and canopy coverage of shrubs showed a slight increment
483 compared to the other two forests, though LAI was decreasing. During this period,
484 interannual throughfall ratio and stemflow ratio showed significantly change over time
485 (Fig. 3), implying the role of interannual variation of forest structure in rainfall
486 redistribution process.

487 Secondly, ongoing rainfall changes with different magnitude favor the different
488 levels of rainfall redistribution over time (Lian et al., 2022). At event scale, throughfall
489 and stemflow proportions of forests were both low with rainfall events <10 mm. The
490 variations of throughfall and stemflow were both larger for gross rainfall <10 mm than
491 events >10 mm. Rainfall threshold associated with the canopy interception capacity had
492 impact on throughfall and stemflow generation (Zabret et al., 2018; André et al., 2008;
493 Durocher, 1990). After the raindrop capacity of the canopy reached its peak, throughfall
494 and stemflow were documented to match the gross rainfall. Therefore, relatively low
495 proportions and high spatial variability appeared before rainfall threshold, and after that,
496 relatively high proportions and low variability until a stable level were observed in the
497 three forests. Moreover, at interannual scale, the raining days in different magnitudes
498 presented obvious fluctuation over 22 years (Fig. 1). This fluctuation of raining days
499 and its magnitude distribution potentially regulated the long-term changes of open
500 rainfall partitioned to interception loss, throughfall and stemflow. Consequently,
501 throughfall and stemflow, influenced by the comprehensive effect of rainfall regimes
502 and forest structures, presented spatiotemporal variability at different level (Fig. 3–6).
503 From a long-term perspective, changing in rainfall redistribution potentially makes
504 forest water and biogeochemistry budget more complex. Further knowledge of the
505 long-term accumulative effect of rainfall redistribution on forest water and chemistry
506 (e.g., soil and plant) is needed in the future.

507 Throughfall and stemflow are part of rainfall and are key player in the water cycle
508 process. Based on the connection of the water cycle to precipitation and temperature
509 and under the background of climate change, frequency of extreme events (heavy
510 rainfall, droughts) needs to be anticipated in the effect on rainfall redistribution and

511 solute transport within forests, which in turn may affect the water cycle and
512 biogeochemical cycles (Blume et al., 2022). In this study, it should be noted that the
513 2008 rainfall data can be used as an example under extreme event. In 2008, extreme
514 weather events occurred in South China. Freezing events occurred in the dry season,
515 continuous heavy rain and typhoon events occurred in the wet season. Gross rainfall
516 was larger than other years, with the annual rainfall of 2361.1 mm (22-year average
517 annual rainfall of 1848.6 mm) (Fig. 1). At the same time, a total of 26 throughfall events
518 were collected in 2008. According to the M-K test, the throughfall and stemflow trend
519 of different forests presented different degree of disturbance under the background of
520 mutation of open rainfall (Fig. 2). In this process, the driving effect of forest structure
521 and rainfall on throughfall and stemflow mutation is synchronous. More data and
522 modeling are needed to support the relevant study about effect of climate change on
523 rainfall redistribution in the future.

524

525 **5. Conclusion**

526 The current study investigated long-term changing characteristic of rainfall
527 redistribution along a subtropical forest succession sequence with: pine forest (PF),
528 mixed pine and broadleaf forest (MF) and monsoon evergreen broadleaf forest (BF).
529 Firstly, in the valid 740 rainfall events throughfall ratio showed in order $BF < MF < PF$,
530 and stemflow ratio showed in order $BF > MF > PF$. The variation of stemflow was
531 higher ($CV > 50\%$) than that of throughfall ($CV < 25\%$). Secondly, throughfall and
532 stemflow of forests experienced a decreasing followed by an increasing from 2001–
533 2022 (except stemflow of the pine forest), similar with the trend of open rainfall. Driven
534 by rainfall and forest factors, interannual variability of both throughfall and stemflow
535 in the broadleaf forest were greater than those in the mixed forest and pine forest, which
536 was different from that of annual open rainfall.

537 For rainwater chemistry, differences of the clement flux in throughfall and
538 stemflow among the three forest types were confirmed based on data from 2001, 2010
539 and 2022. On average, TN and TP fluxes of throughfall presented in order $BF < MF <$
540 PF , while K^+ flux of throughfall presented in order $BF > MF > PF$. Over time, rainwater
541 chemical concentrations were lower in the wet season than that in the dry season. Given
542 the smaller proportion of open rainfall, stemflow chemical fluxes varied less among
543 forest types and/or over time, though tree species exactly contribute to differences in
544 stemflow chemistry. Nevertheless, its funnel effect on soil and plant over time still

545 deserves more attention in the future.

546 The above results indicate that the water volume and chemistry in rainfall
547 redistribution process under forest represented not exactly the same trend as open
548 rainfall over time, and throughfall and stemflow depend on the effect of rainfall and
549 forest factors. This study thus provided insight into the rainfall redistribution process
550 by linking the long-term change of rainfall pattern with a subtropical forest succession
551 sequence.

552

553

554 *Code and data availability.* The data used to derive to the conclusions of the present
555 study are freely accessible. All the data were obtained from the CNERN dataset
556 (<http://dhf.cern.ac.cn/meta/metaData>).

557

558 *Author contributions.* WJZ: conceptualization, investigation, data analysis, writing,
559 visualization. TS and SS: reviewing, supervision. QMZ and CGW: resources, data
560 curation, WLH: reviewing, JXL and XX: reviewing, funding acquisition, supervision

561

562 *Competing interests.* The authors declare that they have no conflict of interest.

563

564 *Disclaimer.* Publisher's note: Copernicus Publications remains neutral with regard to
565 jurisdictional claims made in the text, published maps, institutional affiliations, or any
566 other geographical representation in this paper. While Copernicus Publications makes
567 every effort to include appropriate place names, the final responsibility lies with the
568 authors.

569

570 *Acknowledgements.* Wanjun Zhang would like to acknowledge the financial support
571 from the CSC Fellowship.

572

573 *Financial support.* This research has been supported by The Key-Area Research and
574 Development Program of Guangdong Province (Grant No. 2022B1111230001), the
575 National Natural Science Foundation of China (Grant Nos. 42207158 and 32101342)
576 and the China Postdoctoral Science Foundation (Grant Nos. 2021M703259, 2021
577 M703260, 2021M693220).

578

580 **References**

- 581 André, F., Jonard, M., Jonard, F., Ponette, Q., 2011. Spatial and temporal patterns of throughfall volume
 582 in a deciduous mixed-species stand. *J. Hydrol.* 400(1–2), 244–254.
 583 <https://doi.org/10.1016/j.jhydrol.2011.01.037>
- 584 André, F., Jonard, M., Ponette, Q. (2008). Influence of species and rain event characteristics on stemflow
 585 volume in a temperate mixed oak–beech stand. *Hydrol. Process.* 22(22), 4455–4466.
 586 <https://doi.org/10.1002/hyp.7048>
- 587 Blume, T., Schneider, L., Güntner, A., 2022. Comparative analysis of throughfall observations in six
 588 different forest stands: Influence of seasons, rainfall-and stand characteristics. *Hydrol. Process.*
 589 36(3), e14461. <https://doi.org/10.1002/hyp.14461>
- 590 Borghetti, M., Gentilesca, T., Leonardi, S., Van Noije, T., Rita, A., 2017. Long-term temporal
 591 relationships between environmental conditions and xylem functional traits: a meta-analysis across
 592 a range of woody species along climatic and nitrogen deposition gradients. *Tree Physiol.* 37(1), 4-
 593 17.
- 594 Brasil, J.B., Andrade, E.M.d., Palácio, H.A.d.Q., Medeiros, P.H.A., Santos, J.C.N.d., 2018.
 595 Characteristics of precipitation and the process of interception in a seasonally dry tropical forest. *J.*
 596 *Hydrol-Reg. Stud.* 19, 307–317. <https://doi.org/10.1016/j.ejrh.2018.10.006>
- 597 Brauman, K.A., Freyberg, D.L., Daily, G.C., 2010. Forest structure influences on rainfall partitioning
 598 and cloud interception: A comparison of native forest sites in Kona, Hawai'i. *Agric. For. Meteorol.*
 599 150(2), 265–275. <https://doi.org/10.1016/j.agrformet.2009.11.011>
- 600 Bruijnzeel, L.A., Mulligan, M., Scatena, F.N., 2011. Hydrometeorology of tropical montane cloud forests:
 601 emerging patterns. *Hydrol. Process.* 25(3), 465–498. <https://doi.org/10.1002/hyp.7974>
- 602 Carlyle-Moses, D.E., Laureano, J.F., Price, A.G., 2004. Throughfall and throughfall spatial variability in
 603 Madrean oak forest communities of northeastern Mexico. *J. Hydrol.* 297(1–4), 124–135.
 604 <https://doi.org/10.1016/j.jhydrol.2004.04.007>
- 605 Chen, S., Cao, R., Yoshitake, S., Ohtsuka, T., 2019. Stemflow hydrology and DOM flux in relation to
 606 tree size and rainfall event characteristics. *Agric. For. Meteorol.* 279, 107753.
 607 <https://doi.org/10.1016/j.agrformet.2019.107753>
- 608 Crockford, R.H., Richardson, D.P., 1990. Partitioning of rainfall in a eucalypt forest and pine plantation
 609 in southeastern Australia: II Stemflow and factors affecting stemflow in a dry sclerophyll eucalypt
 610 forest and a *Pinus radiata* plantation. *Hydrol. Process.* 4(2), 145–155.
 611 <https://doi.org/10.1002/hyp.3360040205>
- 612 De Schrijver, A., Geudens, G., Augusto, L., Staelens, J., Mertens, J., Wuyts, K., Gielis, L., Verheyen, K.
 613 (2007). The effect of forest type on throughfall deposition and seepage flux: a review. *Oecologia*,
 614 153, 663-674. <https://doi.org/10.1007/s00442-007-0776-1>
- 615 Dunkerley, D., 2014. Stemflow on the woody parts of plants: dependence on rainfall intensity and event
 616 profile from laboratory simulations. *Hydrol. Process.* 28(22), 5469–5482.
 617 <https://doi.org/10.1002/hyp.10050>
- 618 Durocher, M.G., 1990. Monitoring spatial variability of forest interception. *Hydrol. Process.* 4(3), 215–

619 229. <https://doi.org/10.1002/hyp.3360040303>

620 Exler, J.L., Moore, R.D., 2022. Quantifying throughfall, stemflow and interception loss in five vegetation
621 communities in a maritime raised bog. *Agric. For. Meteorol.* 327, 109202.
622 <https://doi.org/10.1016/j.agrformet.2022.109202>

623 Fan, Y.X., Lu, S.X., He, M., Yang, L.M., Hu, W.F., Yang, Z.J., Liu, X.F., Hui, D.F., Guo, J.F., Yang, Y.S.,
624 2021. Long-term throughfall exclusion decreases soil organic phosphorus associated with reduced
625 plant roots and soil microbial biomass in a subtropical forest. *Geoderma*, 404, 115309.
626 <https://doi.org/10.1016/j.geoderma.2021.115309>

627 Germer, S., Elsenbeer, H., Moraes, J.M., 2006. Throughfall and temporal trends of rainfall redistribution
628 in an open tropical rainforest, south-western Amazonia (Rondônia, Brazil). *Hydrol. Earth Syst. Sci.*
629 10(3), 383–393. <https://doi.org/10.5194/hess-10-383-2006>

630 Germer, S., Neill, C., Krusche, A.V., Neto, S.C.G., Elsenbeer, H., 2007. Seasonal and within-event
631 dynamics of rainfall and throughfall chemistry in an open tropical rainforest in Rondônia, Brazil.
632 *Biogeochemistry*, 86, 155–174. <https://doi.org/10.1007/s10533-007-9152-9>

633 Germer, S., Werther, L., Elsenbeer, H., 2010. Have we underestimated stemflow? Lessons from an open
634 tropical rainforest. *J. Hydrol.* 395(3-4), 169–179. <https://doi.org/10.1016/j.jhydrol.2010.10.022>

635 Goebes, P., Bruelheide, H., Härdtle, W., Kröber, W., Kühn, P., Li, Y., Seitz, S., von Oheimb, G., Scholten,
636 T., 2015. Species-specific effects on throughfall kinetic energy in subtropical forest plantations are
637 related to leaf traits and tree architecture. *PLoS one*, 10(6), e0128084.
638 <https://doi.org/10.1371/journal.pone.0128084>

639 Grunicke, S., Queck, R., Bernhofer, C., 2020. Long-term investigation of forest canopy rainfall
640 interception for a spruce stand. *Agric. For. Meteorol.* 292, 108125.
641 <https://doi.org/10.1016/j.agrformet.2020.108125>

642 Grossiord, C., Sevanto, S., Dawson, T. E., Adams, H.D., Collins, A.D., Dickman, L.T., Newman B.D.,
643 Stockton, E.A., McDowell, N.G. (2017). Warming combined with more extreme precipitation
644 regimes modifies the water sources used by trees. *New Phytol.* 213(2), 584–596.
645 <https://doi.org/10.1111/nph.14192>

646 Huang, W.J., Zhou, G.Y., Liu, J.X., 2012. Nitrogen and phosphorus status and their influence on
647 aboveground production under increasing nitrogen deposition in three successional forests. *Acta*
648 *Oecologica*, 44, 20–27. <https://doi.org/10.1016/j.actao.2011.06.005>

649 Iida, S.I., Tanaka, T., Sugita, M., 2005. Change of interception process due to the succession from
650 Japanese red pine to evergreen oak. *J. Hydrol.* 315(1–4), 154–166.
651 <https://doi.org/10.1016/j.jhydrol.2005.03.024>

652 Jackson, N.A., 2000. Measured and modelled rainfall interception loss from an agroforestry system in
653 Kenya. *Agric. For. Meteorol.* 100, 323–336. [https://doi.org/10.1016/S0168-1923\(99\)00145-8](https://doi.org/10.1016/S0168-1923(99)00145-8)

654 Ji, S.Y., Omar, S.I., Zhang, S.B, Wang, T.F, Chen, C.F, Zhang, W.J., 2022. Comprehensive evaluation of
655 throughfall erosion in the banana plantation. *Earth Surf. Proc. Land.*, 47(12), 2941–2949.
656 <https://doi.org/10.1002/esp.5435>

657 Jiang, Z.Y., Zhi, Q.Y., Van Stan, J.T., Zhang, S.Y., Xiao, Y.H., Chen, X.Y., Wu, H.W., 2021. Rainfall
658 partitioning and associated chemical alteration in three subtropical urban tree species. *J. Hydrol.*

659 603, 127109. <https://doi.org/10.1016/j.jhydrol.2021.127109>

660 Junior, J.J., Mello, C.R., Owens, P.R., Mello, J.M., Curi, N., Alves, G.J., 2017. Time-stability of soil
661 water content (SWC) in an Atlantic Forest-Latosol site. *Geoderma*, 288, 64–78.
662 <https://doi.org/10.1016/j.geoderma.2016.10.034>

663 Keim, R.F., Tromp-van Meerveld, H.J., McDonnell, J.J., 2006. A virtual experiment on the effects of
664 evaporation and intensity smoothing by canopy interception on subsurface stormflow generation. *J.*
665 *Hydrol.* 327(3–4), 352–364. <https://doi.org/10.1016/j.jhydrol.2005.11.024>

666 Klos, P.Z., Chain-Guadarrama, A., Link, T.E., Finegan, B., Vierling, L.A., Chazdon, R., 2014.
667 Throughfall heterogeneity in tropical forested landscapes as a focal mechanism for deep percolation.
668 *J. Hydrol.* 519, 2180–2188. <https://doi.org/10.1016/j.jhydrol.2014.10.004>

669 Kottek, M., Grieser, J., Beck, C., Rudolf, B., Rubel, F., 2006. World map of the Köppen-Geiger climate
670 classification updated. *Meteorologische Zeitschrift*, 15(3), 259–263. [https://doi.org/10.1127/0941-](https://doi.org/10.1127/0941-2948/2006/0130)
671 [2948/2006/0130](https://doi.org/10.1127/0941-2948/2006/0130)

672 Lacombe, G., Valentin, C., Sounyafong, P., De Rouw, A., Soulileuth, B., Silvera, N., Pierret, A.,
673 Sengtaheuanghoung, O., Ribolzi, O., 2018. Linking crop structure, throughfall, soil surface
674 conditions, runoff and soil detachment: 10 land uses analyzed in Northern Laos. *Sci. Total Environ.*
675 616, 1330–1338. <https://doi.org/10.1016/j.scitotenv.2017.10.185>

676 Legout, A., van Der Heijden, G., Jaffrain, J., Boudot, J. P., Ranger, J., 2016. Tree species effects on
677 solution chemistry and major element fluxes: A case study in the Morvan (Breuil, France). *Forest*
678 *Ecol Manag.* 378, 244–258. <https://doi.org/10.1016/j.foreco.2016.07.003>

679 Leuzinger, S., Körner, C., 2010. Rainfall distribution is the main driver of runoff under future CO₂-
680 concentration in a temperate deciduous forest. *Global Change Biol.* 16(1), 246–254.
681 <https://doi.org/10.1111/j.1365-2486.2009.01937.x>

682 Levia, D. F., Nanko, K., Amasaki, H., Giambelluca, T. W., Hotta, N., Iida, S. I., Mudd, R.G., Nullet, M.A.,
683 Sakai, N., Shinori, Y., Sun X.C., Suzuki, M., Tanaka, N., Tantasirin, C., Yamada, K., 2019.
684 Throughfall partitioning by trees. *Hydrol. Process.* 33(12), 1698–1708.
685 <https://doi.org/10.1002/hyp.13432>

686 Levia, D.F., Germer, S., 2015. A review of stemflow generation dynamics and stemflow-environment
687 interactions in forests and shrublands. *Rev. Geophys.* 53(3), 673–714.
688 <https://doi.org/10.1002/2015RG000479>

689 Levia Jr, D.F., Frost, E.E., 2006. Variability of throughfall volume and solute inputs in wooded
690 ecosystems. *Prog. Phys. Geog.* 30(5), 605–632. <https://doi.org/10.1177/0309133306071145>

691 Li, Y., Niu, S.L, Yu, G.R., 2016. Aggravated phosphorus limitation on biomass production under
692 increasing nitrogen loading: a meta-analysis. *Global Change Biol.* 22(2), 934–943.
693 <https://doi.org/10.1111/gcb.13125>

694 Lian, X., Zhao, W.L., Gentine, P., 2022. Recent global decline in rainfall interception loss due to altered
695 rainfall regimes. *Nat. Commun.* 13(1), 7642. <https://doi.org/10.1038/s41467-022-35414-y>

696 Liu, J.Q., Liu, W.J., Li, W.X., Zeng, H.H., 2019. How does a rubber plantation affect the spatial variability
697 and temporal stability of throughfall? *Hydrol. Res.* 50(1), 60–74.
698 <https://doi.org/10.2166/nh.2018.028>

699 Livesley, S.J., Baudinette, B., Glover, D., 2014. Rainfall interception and stem flow by eucalypt street
700 trees – The impacts of canopy density and bark type. *Urban For. Urban Gree.* 13(1), 192–197.
701 <https://doi.org/10.1016/j.ufug.2013.09.001>

702 Llorens, P., Domingo, F., 2007. Rainfall partitioning by vegetation under Mediterranean conditions. A
703 review of studies in Europe. *J. Hydrol.* 335(1–2), 37–54.
704 <https://doi.org/10.1016/j.jhydrol.2006.10.032>

705 Llorens, P., Latron, J., Carlyle-Moses, D.E., Nätthe, K., Chang, J.L., Nanko, K., Lida, S., Levia, D.F.,
706 2022. Stemflow infiltration areas into forest soils around American beech (*Fagus grandifolia* Ehrh.)
707 trees. *Ecohydrology* 15(2), e2369. <https://doi.org/10.1002/eco.2369>

708 Loustau, D., Berbigier, P., Granier, A., 1992. Interception loss, throughfall and stemflow in a maritime
709 pine stand. II. An application of Gash's analytical model of interception. *J. Hydrol.* 138(3–4), 469–
710 485. [https://doi.org/10.1016/0022-1694\(92\)90131-E](https://doi.org/10.1016/0022-1694(92)90131-E)

711 Marin, C.T., Bouten, W., Sevink, J., 2000. Gross rainfall and its partitioning into throughfall, stemflow
712 and evaporation of intercepted water in four forest ecosystems in western Amazonia. *J. Hydrol.*
713 237(1–2), 40–57. [https://doi.org/10.1016/S0022-1694\(00\)00301-2](https://doi.org/10.1016/S0022-1694(00)00301-2)

714 Moslehi, M., Habashi, H., Khormali, F., Ahmadi, A., Brunner, I., Zimmermann, S., 2019. Base cation
715 dynamics in rainfall, throughfall, litterflow and soil solution under Oriental beech (*Fagus orientalis*
716 Lipsky) trees in northern Iran. *Ann. Forest Sci.* 76(2), 1–12. <https://doi.org/10.1007/s13595-019-0837-8>

718 Muzyło, A., Llorens, P., Domingo, F., 2012. Rainfall partitioning in a deciduous forest plot in leafed and
719 leafless periods. *Ecohydrology*, 5(6), 759–767. <https://doi.org/10.1002/eco.266>

720 Nanko, K., Hotta, N., Suzuki, M., 2006. Evaluating the influence of canopy species and meteorological
721 factors on throughfall drop size distribution. *J. Hydrol.* 329(3–4), 422–431.
722 <https://doi.org/10.1016/j.jhydrol.2006.02.036>

723 Niu, X.T., Fan, J., Du, M.G., Dai, Z.J., Luo, R.H., Yuan, H.Y., Zhang, S.G., 2023. Changes of Rainfall
724 Partitioning and canopy interception modeling after progressive thinning in two shrub plantations
725 on the Chinese Loess Plateau. *J. Hydrol.* 619, 129299.
726 <https://doi.org/10.1016/j.jhydrol.2023.129299>

727 Pinos, J., Latron, J., Levia, D. F., Llorens, P., 2021. Drivers of the circumferential variation of stemflow
728 inputs on the boles of *Pinus sylvestris* L. (Scots pine). *Ecohydrology*, 14(8), e2348.

729 Ponette-González, A.G., Weathers, K.C., Curran, L.M., 2010. Water inputs across a tropical montane
730 landscape in Veracruz, Mexico: synergistic effects of land cover, rain and fog seasonality, and
731 interannual precipitation variability. *Global Change Biol.* 16(3), 946–963.
732 <https://doi.org/10.1111/j.1365-2486.2009.01985.x>

733 Price, A.G., Dunham, K., Carleton, T., Band, L., 1997. Variability of water fluxes through the black
734 spruce (*Picea mariana*) canopy and feather moss (*Pleurozium schreberi*) carpet in the boreal forest
735 of Northern Manitoba. *J. Hydrol.* 196(1–4), 310–323. [https://doi.org/10.1016/S0022-1694\(96\)03233-7](https://doi.org/10.1016/S0022-1694(96)03233-7)

737 Reynaert, S., De Boeck, H.J., Verbruggen, E., Verlinden, M., Flowers, N., Nijs, I., 2021. Risk of short-
738 term biodiversity loss under more persistent precipitation regimes. *Global Change Biol.* 27(8),

739 1614–1626. <https://doi.org/10.1111/gcb.15501>

740 Rodrigues, A.F., Terra, M.C., Mantovani, V.A., Cordeiro, N.G., Ribeiro, J.P., Guo, L., Nehren, U., Mello,
741 M.J., Mello, C.R., 2022. Throughfall spatial variability in a neotropical forest: Have we correctly
742 accounted for time stability? *J. Hydrol.* 608, 127632. <https://doi.org/10.1016/j.jhydrol.2022.127632>

743 Seiler, J., Matzner, E., 1995. Spatial variability of throughfall chemistry and selected soil properties as
744 influenced by stem distance in a mature Norway spruce (*Picea abies*, Karst.) stand. *Plant Soil* 176,
745 139–147. <https://doi.org/10.1007/BF00017684>

746 Shen, W.J., Ren, H.L., Jenerette, G.D., Hui, D.F., Ren, H., 2013. Atmospheric deposition and canopy
747 exchange of anions and cations in two plantation forests under acid rain influence. *Atmos Environ.*
748 64, 242–250. <https://doi.org/10.1016/j.atmosenv.2012.10.015>

749 Shinohara, Y., Levia, D.F., Komatsu, H., Nogata, M., Otsuki, K., 2015. Comparative modeling of the
750 effects of intensive thinning on canopy interception loss in a Japanese cedar (*Cryptomeria japonica*
751 D. Don) forest of western Japan. *Agric. For. Meteorol.* 214–215, 148–156.
752 <https://doi.org/10.1016/j.agrformet.2015.08.257>.

753 Siegert, C.M., Levia, D.F., 2014. Seasonal and meteorological effects on differential stemflow funneling
754 ratios for two deciduous tree species. *J. Hydrol.* 519, 446–454.
755 <https://doi.org/10.1016/j.jhydrol.2014.07.038>

756 Staelens, J., De Schrijver, A., Verheyen, K., 2007. Seasonal variation in throughfall and stemflow
757 chemistry beneath a European beech (*Fagus sylvatica*) tree in relation to canopy phenology. *Can. J.*
758 *Forest Res.* 37(8), 1359–1372. <https://doi.org/10.1139/X07-003>

759 Staelens, J., De Schrijver, A., Verheyen, K., Verhoest, N.E., 2006. Spatial variability and temporal
760 stability of throughfall deposition under beech (*Fagus sylvatica* L.) in relationship to canopy
761 structure. *Environ. Pollut.* 142(2), 254–263. <https://doi.org/10.1016/j.envpol.2005.10.002>

762 Su, L., Zhao, C.M., Xu, W.T., Xie, Z.Q., 2019. Hydrochemical fluxes in bulk precipitation, throughfall,
763 and stemflow in a mixed evergreen and deciduous broadleaved forest. *Forests* 10(6), 507.
764 <https://doi.org/10.3390/f10060507>

765 Sun, J.M., Yu, X.X., Wang, H.N., Jia, G.D., Zhao, Y., Tu, Z.H., Deng, W.P., Jia, J.B., Chen, J.G., 2018.
766 Effects of forest structure on hydrological processes in China. *J. Hydrol.* 561, 187–199.
767 <https://doi.org/10.1016/j.jhydrol.2018.04.003>

768 Sun, S.Y., Liu, X.F., Lu, S.X., Cao, P.L., Hui, D.F., Chen, J., Guo, J.F., Yang, Y.S., 2023. Depth-dependent
769 response of particulate and mineral-associated organic carbon to long-term throughfall reduction in
770 a subtropical natural forest. *Catena*, 223, 106904. <https://doi.org/10.1016/j.catena.2022.106904>

771 Tonello, K.C., Rosa, A.G., Pereira, L.C., Matus, G.N., Guandique, M.E.G., Navarrete, A.A., 2021a.
772 Rainfall partitioning in the Cerrado and its influence on net rainfall nutrient fluxes. *Agric. For.*
773 *Meteorol.* 303, 108372. <https://doi.org/10.1016/j.agrformet.2021.108372>

774 Tonello, K.C., Van Stan II, J.T., Rosa, A.G., Balbinot, L., Pereira, L.C., Bramorski, J., 2021b. Stemflow
775 variability across tree stem and canopy traits in the Brazilian Cerrado. *Agric. For. Meteorol.* 308,
776 108551. <https://doi.org/10.1016/j.agrformet.2021.108551>

777 Turpault, M.P., Kirchen, G., Calvaruso, C., Redon, P.O., Dincher, M., 2021. Exchanges of major elements
778 in a deciduous forest canopy. *Biogeochemistry*, 152, 51–71. [23](https://doi.org/10.1007/s10533-020-</p>
</div>
<div data-bbox=)

779 00732-0

780 Wu, T., Song, Y.T., Tissue, D., Su, W., Luo, H.Y., Li, X., Yang, S.M., Liu, X.J., Yan J.H., Huang, J., Liu,
781 J.X., 2023. Photosynthetic and biochemical responses of four subtropical tree seedlings to reduced
782 dry season and increased wet season precipitation and variable N deposition. *Tree Physiol.* tpad114.

783 Wu, Y.P., Yin, X.W., Zhou, G.Y., Bruijnzeel, L. A., Dai, A.G., Wang, F., Gentine, P., Zhang, G.C., Song,
784 Y.N., Zhou, D.C., 2024. Rising rainfall intensity induces spatially divergent hydrological changes
785 within a large river basin. *Nat. Commun.* 15(1), 823. <https://doi.org/10.1038/s41467-023-44562-8>

786 Van Stan II, J.T., Pypker, T.G., 2015. A review and evaluation of forest canopy epiphyte roles in the
787 partitioning and chemical alteration of precipitation. *Sci. Total Environ.* 536, 813–824.
788 <https://doi.org/10.1016/j.scitotenv.2015.07.134>

789 Van Stan, J.T., Wagner, S., Guillemette, F., Whitetree, A., Lewis, J., Silva, L., Stubbins, A., 2017.
790 Temporal dynamics in the concentration, flux, and optical properties of tree-derived dissolved
791 organic matter in an epiphyte-laden oak-cedar forest. *J. Geophys. Res-Bioge.* 122(11), 2982–2997.
792 <https://doi.org/10.1002/2017JG004111>

793 Wang, C.Y., Sun, X.C., Fan, C.B., Wei, Y.X., Jia, G.K., Cao, Y.H., 2023. Spatio-temporal variability and
794 intra-event variation of throughfall ammonium and nitrate in a pine plantation. *Hydrol. Process.*
795 e14872. <https://doi.org/10.1002/hyp.14872>

796 Yan, J.H., Zhou, G.Y., Zhang, D.Q., Wang, X., 2003. Spatial and temporal variations of some
797 hydrological factors in a climax forest ecosystem in the Dinghushan region. *Acta Ecologica Sinica*
798 23(11), 2359–2366. <https://europemc.org/article/cba/534217>

799 Yue, K., De Frenne, P., Fornara, D.A., Van Meerbeek, K., Li, W., Peng, X., Ni, X.Y., Peng, Y., Wu, F.Z.,
800 Yang Y.S., Peñuelas, J., 2021. Global patterns and drivers of rainfall partitioning by trees and
801 shrubs. *Global Change Biol.* 27(14), 3350–3357. <https://doi.org/10.1111/gcb.15644>

802 Zabret, K., Rakovec, J., Šraj, M., 2018. Influence of meteorological variables on rainfall partitioning for
803 deciduous and coniferous tree species in urban area. *J. Hydrol.* 558, 29–41.
804 <https://doi.org/10.1016/j.jhydrol.2018.01.025>

805 Zhang, W.J., Zhu, X.A., Chen, C.F., Zeng, H.H., Jiang, X.J., Wu, J.E., Zou, X., Yang, B., Liu, W.J., 2021.
806 Large broad-leaved canopy of banana (*Musa nana* Lour.) induces dramatically high spatial–
807 temporal variability of throughfall. *Hydrol. Res.* 52(6), 1223–1238.
808 <https://doi.org/10.2166/nh.2021.023>

809 Zhang, Y.F., Wang, X.P., Hu, R., Pan, Y.X., Paradeloc, M., 2015. Rainfall partitioning into throughfall,
810 stemflow and interception loss by two xerophytic shrubs within a rain-fed re-vegetated desert
811 ecosystem, northwestern China. *J. Hydrol.* 527, 1084–1095.
812 <https://doi.org/10.1016/j.jhydrol.2015.05.060>

813 Zhang, Y.F., Yuan, C., Chen, N., Levia, D.F., 2023. Rainfall partitioning by vegetation in China: A
814 quantitative synthesis. *J. Hydrol.* 617, 128946. <https://doi.org/10.1016/j.jhydrol.2022.128946>

815 Zhao, W.Y., Ji, X.B., Jin, B.W., Du, Z.Y., Zhang, J.L., Jiao, D.D., Zhao, L.W., 2023. Experimental
816 partitioning of rainfall into throughfall, stemflow and interception loss by *Haloxylon ammodendron*,
817 a dominant sand-stabilizing shrub in northwestern China. *Sci. Total Environ.* 858, 159928.
818 <https://doi.org/10.1016/j.scitotenv.2022.159928>

819 Zheng, M.H., Zhang, T., Luo, Y.Q., Liu, J.X., Lu, X.K., Ye, Q., Wang, S.H., Huang, J., Mao, Q.G., Mo,
820 J.M., Zhang, W., 2022. Temporal patterns of soil carbon emission in tropical forests under long-term
821 nitrogen deposition. *Nat. Geosci.* 15, 1002–1010. <https://doi.org/10.1038/s41561-022-01080-4>
822 Zhou, G.Y., Wei, X.H., Wu, Y.P., Liu, S.G., Huang, Y.H., Yan, J.H., Zhang, D.Q., Zhang, Q.M., Liu, J.X.,
823 Meng, Z., Wang, C.L., Chu, G.W., Liu, S.Z., Tang, X.L., Liu, X.D., 2011. Quantifying the
824 hydrological responses to climate change in an intact forested small watershed in Southern China.
825 *Global Change Biol.* 17(12), 3736–3746. <https://doi.org/10.1111/j.1365-2486.2011.02499.x>
826 Ziegler, A.D., Giambelluca, T.W., Nullet, M.A., Sutherland, R.A., Tantasarin, C., Vogler, J.B., Negishi,
827 J.N., 2009. Throughfall in an evergreen-dominated forest stand in Northern Thailand: comparison
828 of mobile and stationary methods. *Agric. For. Meteorol.* 149, 373–384.
829 <https://doi.org/10.1016/j.agrformet.2008.09.002>.
830 Zimmermann, A., Wilcke, W., Elsenbeer, H., 2007. Spatial and temporal patterns of throughfall quantity
831 and quality in a tropical montane forest in Ecuador. *J. hydrol.* 343(1–2), 80–96.
832 <https://doi.org/10.1016/j.jhydrol.2007.06.012>

833 **Tables**

834

835 **Table 1** Correlations between throughfall and stemflow and rainfall and forest factors

	Gross rainfall	DBH	CA	Height	LAI
Throughfall	0.72***	—	—	—	-0.58**
stemflow	0.77***	0.65*	-0.75**	0.54**	-0.55**

836 DBH: diameter at breast height; CA: crown area; LAI: leaf area index. * $P < 0.05$, ** $P < 0.01$, *** $P <$

837 0.001

838

839

840

841

842

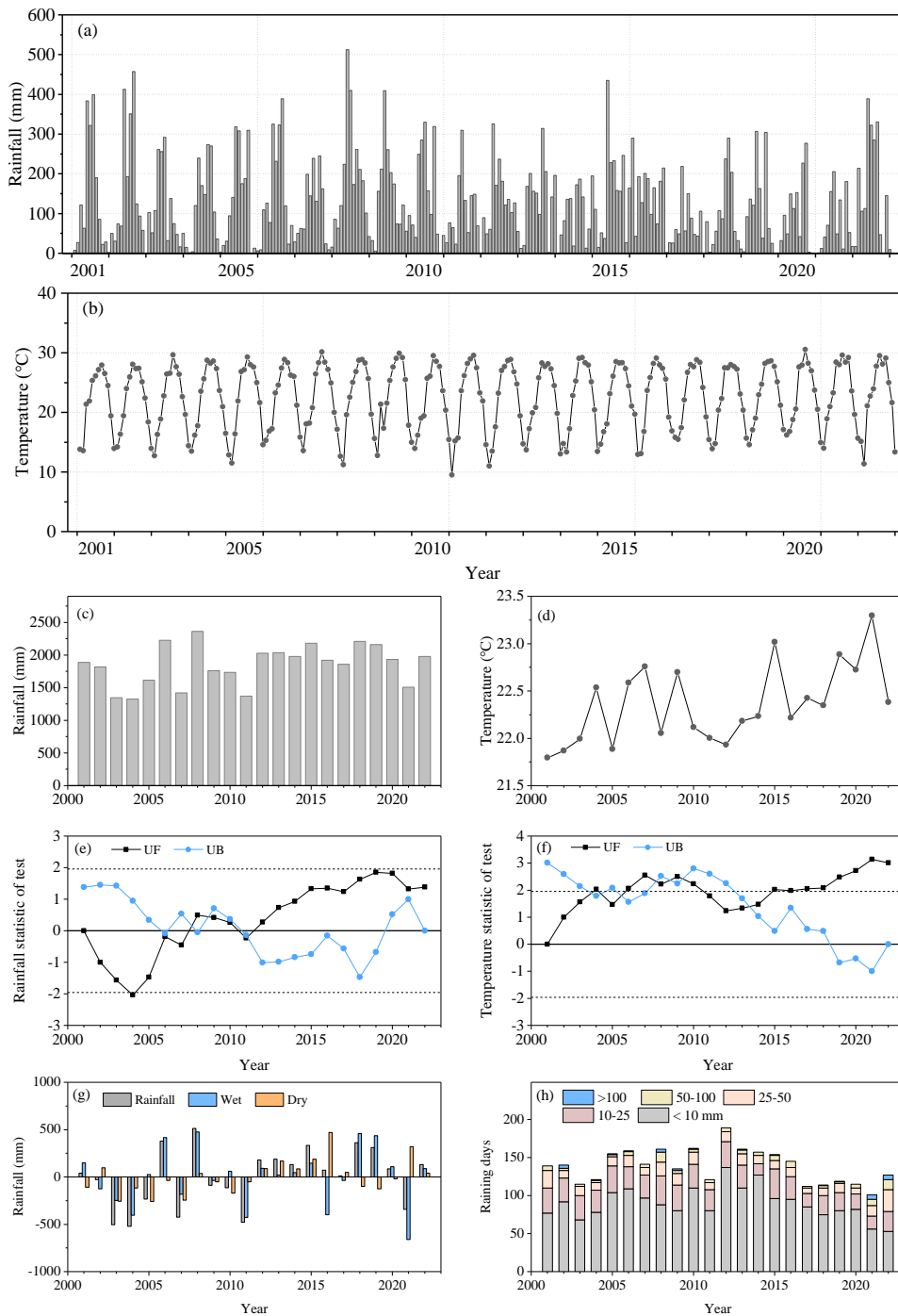
843

844 **Table 2** Analysis of variance (ANOVA) for throughfall and stemflow affected by rainfall
845 classifications and tree species

Summary of ANOVA	Throughfall		Stemflow
Rainfall classification (R)	< 0.05	Rainfall classification (R)	< 0.001
Forest type (F)	< 0.001	Tree species (T)	< 0.001
R × F	0.861	R × T	< 0.001

846 $\alpha = 0.05$

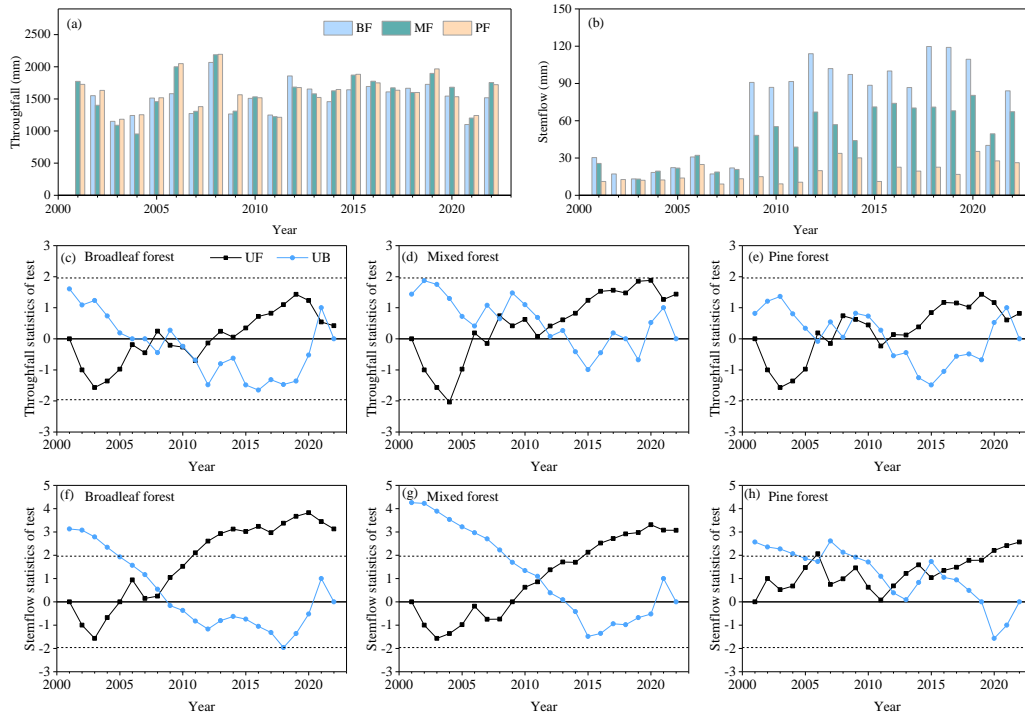
847



849

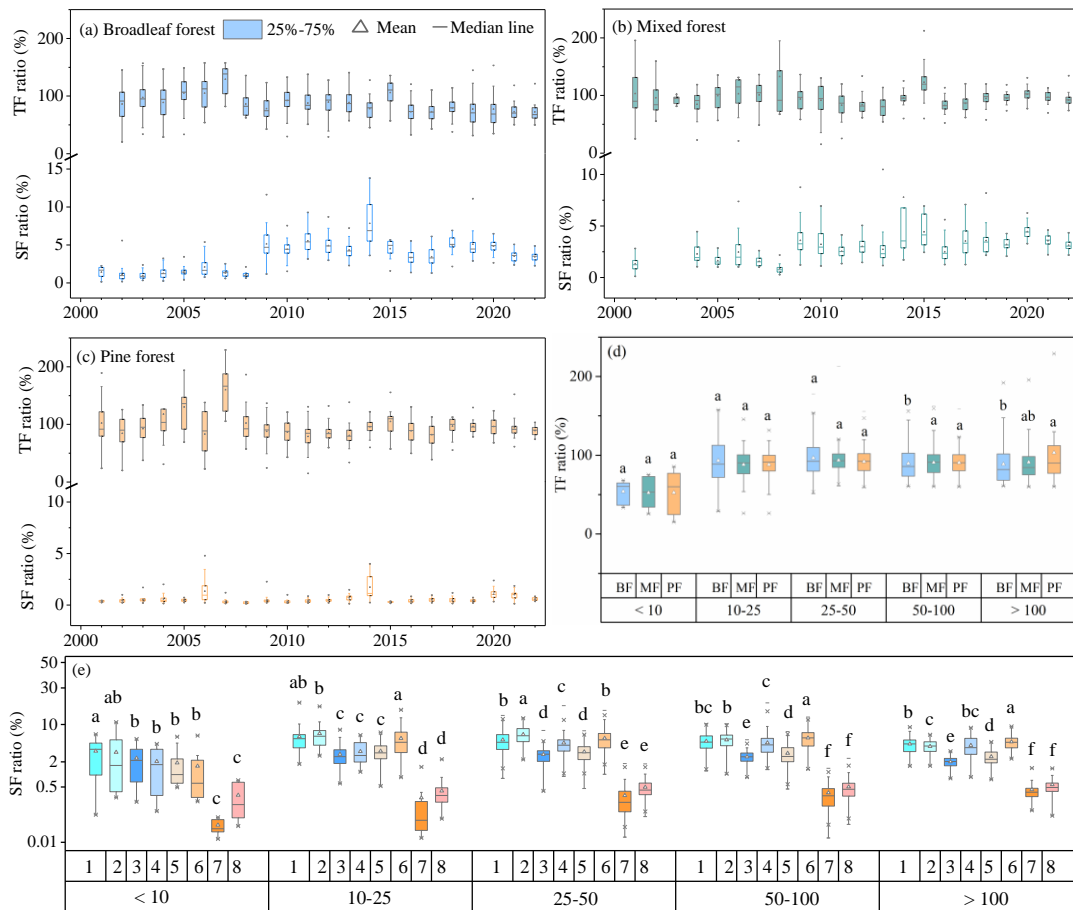
850 **Fig. 1** (a) and (b) rainfall and temperature in Dinghushan Biosphere Reserve in Southern China
 851 from 2001–2022, (c) and (d) annual rainfall and temperature, (e) and (f) rainfall and
 852 temperature statistic of Mann-Kendall test, respectively. (g) Anomaly of annual rainfall from
 853 2001–2022, (h) annual raining days in five classifications. UF (Unadjusted Forward) > 0
 854 indicate a continuous increasing trend ($P < 0.05$). The intersection points of UF and UB
 855 (Unadjusted Backward) is the mutation time point. Within the confidence interval [-1.96, 1.96],
 856 the variable presents a significantly mutation growth state at this time point ($P < 0.05$).

857

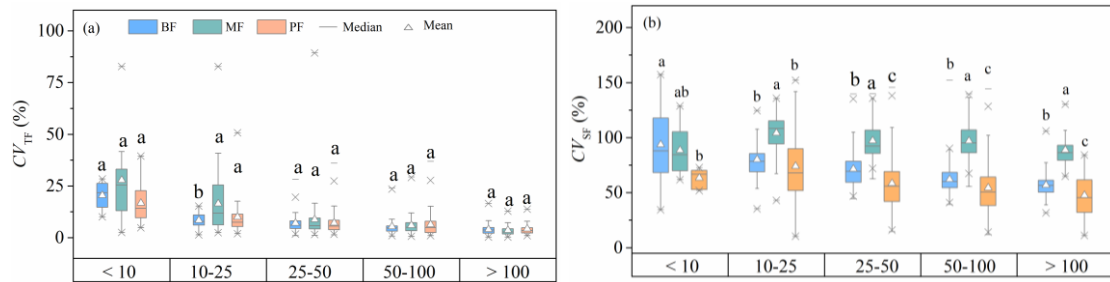


858

859 **Fig. 2** (a) and (b) Annual throughfall and stemflow in the broadleaf forest (BF), mixed pine and
 860 broadleaf forest (MF) and pine forest (PF) from 2001–2022, respectively, (c) ~ (h) rainfall and
 861 stemflow statistic of Mann-Kendall test, respectively. UF (Unadjusted Forward) > 0 indicate a
 862 continuous increasing trend ($P < 0.05$). The intersection points of UF and UB (Unadjusted
 863 Backward) is the mutation time point. Within the confidence interval $[-1.96, 1.96]$, the variable
 864 presents a significantly mutation growth state at this time point ($P < 0.05$).



865
 866 **Fig. 3** Box plots of throughfall ratio and stemflow ratio in (a) broadleaf forest, (b) mixed pine and
 867 broadleaf forest and (c) pine forest from 2001–2022. Boxed plots of (d) TF ratio in the three
 868 forests and (e) SF ratio for eight plant species based on the rainfall classifications (broadleaf
 869 forest: *Acmena acuminatissima* (Blume) Merr. et Perry (SF1), *Cryptocarya chinensis* (Hance)
 870 Hemsl. (SF2), *Gironniera subaequalis* Planch. (SF3), *Schima superba* Gardn. et Champ. (SF4);
 871 mixed forest: *Castanea henryi* (Skam) Rehd. et Wils. (SF5), *Schima superba* Gardn. et Champ.
 872 (SF6), *Pinus massoniana* Lamb. (SF7); pine forest: *Pinus massoniana* Lamb. (SF8). Different
 873 letters indicate a significant difference at $P < 0.05$



875

876

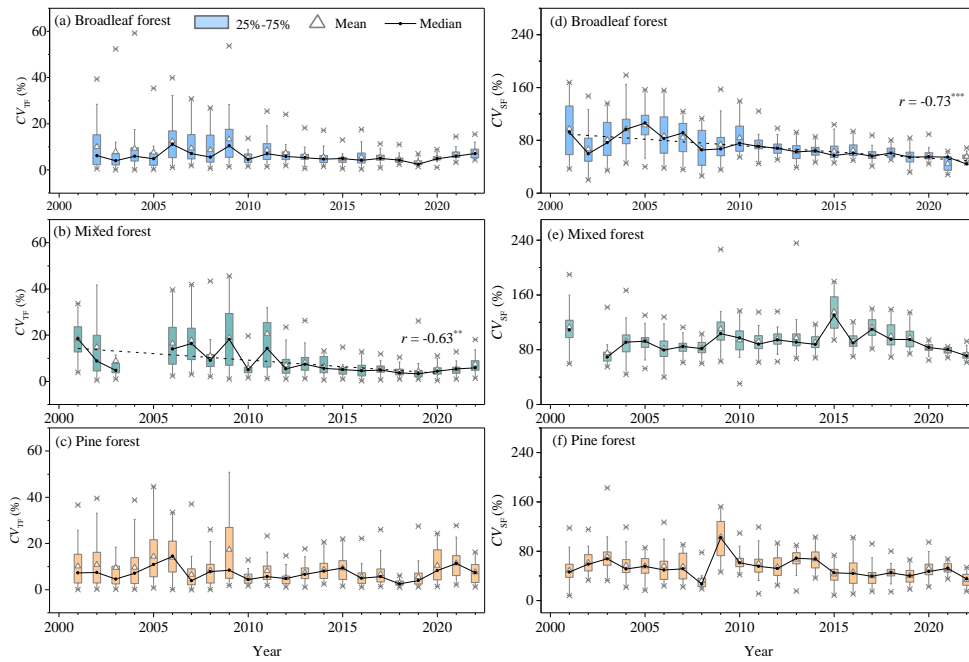
Fig. 4 Box plots of coefficient of variation (CV , %) in (a) throughfall (TF) and (b) stemflow (SF) in

877

broadleaf forest (BF), mixed pine and broadleaf forest (MF) and pine forest (PF) based on the

878

rainfall classifications. Different letters indicate a significant difference at $P < 0.05$

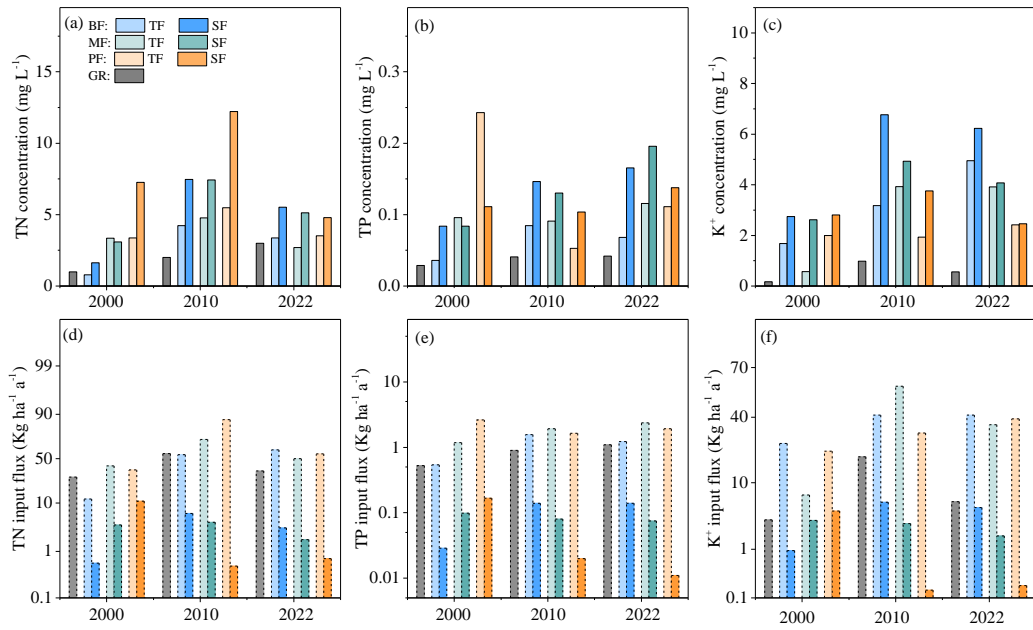


880

881 **Fig. 5** Box plots of coefficient of variation (CV , %) in (a, b, and c) throughfall (TF) and (d, e, and f)

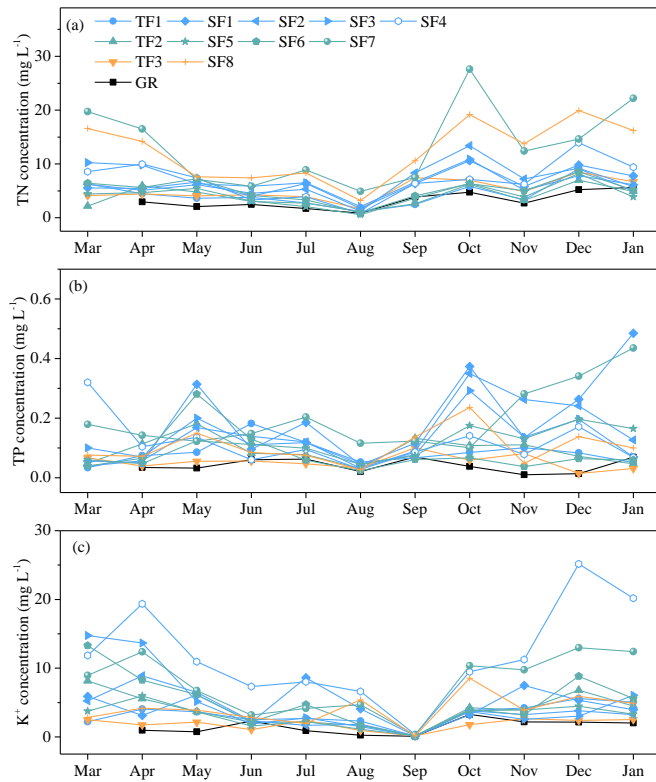
882 stemflow (SF) in the three forests from 2001 to 2022. Medians of annual CV were fitted. r :

883 Pearson coefficient of correlation; *: $P < 0.05$, **: $P < 0.01$, ***: $P < 0.001$



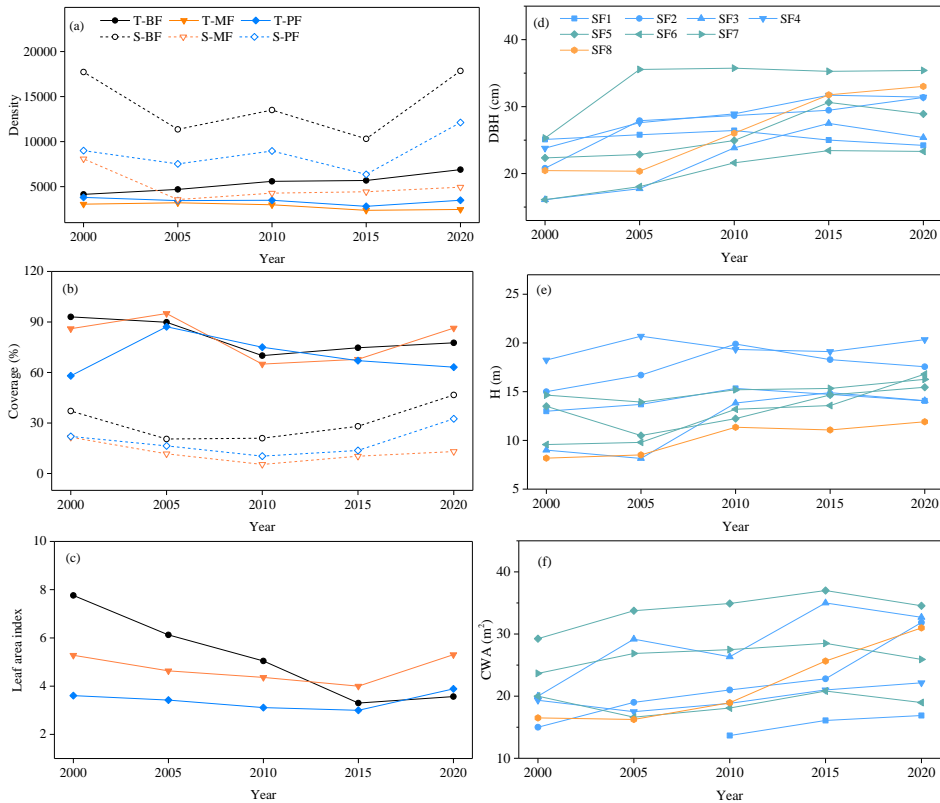
884

885 **Fig. 6** Concentrations and fluxes of TN, TP and K⁺ of gross rainfall (GR), throughfall (TF) and
 886 stemflow (SF) in the broadleaf forest (BF), mixed forest (MF) and pine forest (PF) in 2000,
 887 2010 and 2022, respectively.



888
889
890
891

Fig. 7 Monthly concentrations of (a) TN, (b) TP and (c) K⁺ of throughfall (TF1) and stemflow (SF1, SF2, SF3 and SF4) in the broadleaf forest, throughfall (TF2) and stemflow (SF5, SF6 and SF7) in the mixed forest, throughfall (TF3) and stemflow (SF8) in the pine forest.



892 **Fig. 8** Plant density, canopy coverage and leaf area index of tree (T) and shrub (S) in the broadleaf
 893 forest (BF), mixed forest (MF) and pine forest (PF), respectively. Diameter at breast height
 894 (DBH), height (H) and crown area (CA) is given for eight stemflow-sampled trees, respectively.
 895 Tree height was measured using laser range finder. Tape measure was used to measure the
 896 diameter of trees at a height of 1.3 m, namely DBH (diameter at breast height). CA (crown
 897 area): the laser rangefinder was used to measure the maximum diameter at the edge of the
 898 canopy, with multiple measurements at different points to ensure accuracy. Plant density: 25
 899 plots of 20 m × 20 m (A1-A25 plots) were built on a plot of 1hm² to survey tree density. Then,
 900 25 plots of 5 m × 5 m (B1-B25 plots) were randomly set on the A1-A25 plots to survey shrub
 901 density. Finally, 25 plots of 1 m × 1 m (C1-C25 plots) were randomly set on the B1-B25 plots
 902 to survey herb density. Canopy coverage: 25 observation plots (1 m × 1 m) were selected in
 903 the 1 hm² area of each forest type. The percentage of the surface area covered by plants to the
 904 total plot area is termed canopy coverage (%). LAI (Leaf area index) was measured using a
 905 LAI-2200 plant canopy analyzer with 90° view caps (Li-Cor Inc., USA). 10 observation points
 906 (distance about 10 m) were selected in the 1 hm² area of each forest type with 5 replications.
 907
 908